Am J Transl Res 2025;17(6):4135-4147
www.ajtr.org /ISSN:1943-8141/AJTR0163359

Original Article

Altered expression of TEF gene in childhood constipation leads to a decrease in CD56$^+$ NK cells

Yingying Wang[1*], Ziyi Li[2,3*], Lixiang Li[2,3,4*], Houyan Huang[1], Heqing Cui[5], Lili Zhang[5], Li'e Xiang[5], Sujuan Liu[1], Ye Jiang[1], Ping Xu[1], Taocheng Zhou[1], Hui Peng[2,3], Peisen Wang[2,3], Lili Shang[5]

[1]Department of Pediatrics, Anhui Provincial Children's Hospital, Hefei 230031, Anhui, P. R. China; [2]Department of General Surgery, The First Affiliated Hospital of Anhui University of Chinese Medicine, Hefei 230031, Anhui, P. R. China; [3]Institute of Chinese Medicine Surgery, Anhui Academy of Chinese Medicine, Hefei 230031, Anhui, P. R. China; [4]Department of Hepatobiliary Surgery, Lujiang County People's Hospital, Hefei 231500, Anhui, P. R. China; [5]Department of Pediatrics, The First Affiliated Hospital of Anhui University of Chinese Medicine, Hefei 230031, Anhui, P. R. China. [*]Equal contributors.

Received January 16, 2025; Accepted May 7, 2025; Epub June 15, 2025; Published June 30, 2025

Abstract: Objectives: This study used a quantitative bioinformatic analysis of public RNA sequencing databases to study key molecules mediating the occurrence of childhood constipation (CHC) and explore associated immune cell abnormalities and the role of natural killer (NK) cells. Methods: Gene expression profiling datasets, including CHC (GSE36701), were obtained. Immune genes were downloaded from the MSigDB database, and 3,907 immune-related genes were obtained. Differential analysis and weighted gene co-expression network analysis identified 12 hub genes related to CHC and immune genes in adipose tissue and blood samples from GSE36701. Gene ontology analysis was performed to determine key biologic processes. Stepwise and logistic regression analyses were performed to select specific genes for constructing a diagnostic model for CHC. The model was validated using GSE36701, and its diagnostic performance was assessed using the AUC value. The study recruited 20 CHC patients and 20 HV children. After blood collection, peripheral blood mononuclear cells (PBMCs) were extracted, and flow cytometry was used to detect the proportions of immune cells in the blood. qRT-PCR was employed to measure the expression of hub genes in NK cells. Results: A total of 12 hub genes were identified, among which the regulation of steroid metabolic processes and renal sodium excretion were closely associated with an increased expression level of CHC. Gene set enrichment analysis revealed that the core genes were associated with glycosphingolipid biosynthesis ganglio series, base excision repair, and ribosome characteristics. Immunoinfiltration analysis and experimental findings showed that the proportion of CD56$^+$ NK cells in patients with CHC was significantly lower compared to healthy children. The qRT-PCR results indicated that compared to the healthy volunteers group, the expression of AGTR1, FAM200B, NRSN2-AS1, PRAC1, SERTAD3, and TEF genes was decreased, while the expression of APANXA2-OT1, FM09P, and LOC100506929 genes was increased in the CHC group. Conclusion: This study identified TEF as a hub gene associated with the coexistence of CHC and immune cell abnormalities. The study highlights the important role of CD56$^+$ NK cells in the pathogenesis of CHC and provides possible targets for diagnosis and therapeutic intervention.

Keywords: Childhood constipation, immune cells, TEF, CD56$^+$ NK cells, gene expression profiling, pediatric immunology

Introduction

Childhood constipation (CHC) is one of the most common conditions in children [1]. According to the Rome IV diagnostic criteria released in 2016, the criteria for diagnosis require ≥ 2 of the following indicators: constipation at least once a week for a minimum of one month; ≤ 2 bowel movements per week; ≥ 1 episode of large diameter stool; maintaining painful or severe posture during bowel movements; stool impaction; and large diameter stool that can block the toilet [2]. Studies reported that in infants aged 0-6 months, the incidence of constipation was approximately 1.5%. In infants aged 0-12 months, the prevalence of constipation was 1.3-17.7%. Among children aged 13-48 months, it was 1.3-26%, and in children aged

https://doi.org/10.62347/WZA09129

4-18 years old is it was 13% [3, 4]. The majority of cases (approximately 96%) are attributed to functional causes [5], while organic causes of constipation are rare and can often be excluded clinically [6]. Long-term constipation in children can lead to multiple adverse symptoms, including abdominal pain, bloating, vomiting, loss of appetite, failure to thrive, encopresis (involuntary soiling of underwear), anal fissures, and cystitis (caused by accumulation of fecal matter near the urethra) [7]. However, many previous studies have primarily focused on the disease itself while overlooking any potential connection between constipation and immune cells [8, 9].

Immune cells are broadly classified into specific and non-specific cells. Nonspecific cells include neutrophils, eosinophils, monocytes, macrophages, dendritic cells, and natural killer (NK) cells, while specific immune cells include B and T cells [10, 11]. Normal immune function is essential for maintaining normal body functions. Abnormalities in immune cells and their functions are often caused by changes in the frequency or activation state of specific immune cells or subsets, resulting in corresponding changes in immune molecules in the body and affecting some physiologic functions [12, 13]. Studies have shown a close relationship between T cells and the intestine [14, 15]. For instance, T-helper 17 (Th17) cells can regulate the host's defense and resistance to extracellular pathogens in the skin and mucous membranes, and are widely distributed in the gut lamina propria [16]. Other subsets of $CD4^+$ helper T cells, including Th1, Th2, Th17, and Treg cells, also contribute to immune regulation [17]. When constipation occurs, the rectum is often affected, and studies have shown that the proportion of peripheral Th17 and Treg cells is positively correlated with the severity of colonic involvement [18]. This indicates that there is a connection between the distribution of peripheral T cell subsets and constipation [18]. Although some studies have shown that CHC is associated with abnormal immune cells, few have specifically identified the immune cells that exhibit the most significant alteration in pediatric constipation [19].

Utilizing publicly available data and bioinformatics methods, this study conducted differential analysis and weighted gene co-expression network analysis on GSE36701 data to identify hub genes related to immune function and pediatric constipation. Further gene ontology (GO) and gene set enrichment analysis (GSEA) were performed to explore the biological processes and pathways involved. Two genes were screened using stepwise and logistic regression analyses, leading to the development of a diagnostic model for pediatric constipation. The model was validated using the GSE36701 dataset. The AUC value indicated that the model had good diagnostic performance, suggesting clinical application in the diagnosis of pediatric constipation. As pediatric constipation is associated with immune cell function, we further investigated the immune infiltration and correlation between various immune factors and these hub genes, and verified the abnormalities of these hub genes. To validate these findings, we conducted an analysis of gene abnormalities and immune cell correlations using blood samples from 40 children with pediatric constipation [20]. The results showed a strong correlation between pediatric constipation and NK cell maturation, providing insight for precise treatment and control strategies.

Materials and methods

Data acquisition

Gene expression data were obtained from the National Center for Biotechnology Information Gene Expression Omnibus public database. GSE36701 contained RNA expression data annotated by GPL570 in the rectal biopsies. This dataset included 18 participants with constipation-predominant irritable bowel syndrome (IBS-C) and 27 patients with diarrhea-predominant IBS (IBS-D) compared to 21 healthy volunteers (HV). Additionally, it included 21 cases of *Campylobacter jejuni* infection categorized as post-infectious bowel disease (PIBD), post-infection IBS (PIBS), and post-infection non-IBS (PINIBS), compared with 19 HV. PIBD refers to IBS developing within 6 months after *Campylobacter infection,* PIBS represents post-infection IBS of unknown time point and organism, and PINIBS refers to individuals who experienced *Campylobacter infection* without developing IBS.

Differential expression analysis

Differential expression analysis of IBS-C, IBS-D, and HV samples was performed using the

"limma" package in R software. Genes with an adjusted *P*-value (p_adj) < 0.01 and an absolute log-fold (logFC) > 0.585 were considered differentially expressed genes (DEGs). Heat maps and volcano plots illustrating DEGs were generated using the "pheatmap" and "ggplot2" packages.

Identification of hub genes

To obtain hub genes associated with IBS-C, IBS-D, and HV samples, the intersection of DEGs was determined using the "VennDiagram" package in R software. Differences in the expression levels of hub genes between the IBS-C, IBS-D, and HV samples were represented by violin plots. Statistical comparisons were performed using the t-test for normally distributed data and the Mann-Whitney U test for non-normally distributed data. Statistical significance was defined as $P < 0.05$.

Enrichment analysis

Functional enrichment analyses were conducted to investigate the biological mechanisms by which hub genes affect IBS. First, we analyzed the GO biological processes in which these genes are involved, and the final results were presented in a chord diagram using the "GOplot" package in R software. Next, the functions of each gene were revealed using GSEA. The samples were divided into low and high expression groups based on median values of hub gene expression levels. Genes were sorted by logFC from the highest to the lowest, and the final results were presented using the "enrichplot" package in R software. All these analyses were conducted using the "clusterProfiler" package in R software, and the screening condition was p_adj < 0.05.

Logistic regression model

Logistic regression is a generalized linear regression analysis model that can be used for automatic diagnosis of diseases. In this study, logistic regression with two response variables was used, representing the IBS sample when the response variable was 1 and the HV sample when it was 0. Stepwise regression analysis was used to eliminate factors that were not significant for the response variable, and only those that were significant were retained to simplify the model. Stepwise regression iteratively added or removed variables from the model until the statistical value of the Akaike information criterion was minimized. Subsequently, logistic regression was used to fit the relationship between these significant factors and the response variables. Finally, the diagnostic efficacy of the model was evaluated using receiver operating characteristic curves (ROCs) and the area under the ROC curve as described by Coat et al. (2015) and Lai et al. (2021). These analyses were performed with the "stats" and "pROC" packages in R software.

Immune infiltration and immune-related factors

Immune cell infiltration within the microenvironment was assessed using CIBERSORT, which contains 547 biomarkers and 22 human immune cells, including plasma, B cells, T cells, and myeloid cell subpopulations. This tool is based on the linear support vector regression principle for deconvolution analysis of the expression matrix of immune cells. This study used expression data from GSE36701 to quantify the relative proportions of 22 immune cells in each sample. In addition, Spearman's correlation analysis was performed between hub genes, immune infiltration, and immune factors. This analysis was performed using the "psych" package in R software, and the results were displayed as heatmaps. Different immune factors, including 24 immunoinhibitors, 45 immunostimulators, and 41 chemokines, were downloaded from the TISIDB database (Ru et al., 2019).

Flow cytometry analysis for clinical pediatric immunophenotyping and cell subset proportion determination

We recruited 20 pediatric patients with constipation and 20 healthy children from Anhui Provincial Children's Hospital. Clinical data, including age, sex, and relevant examination indicators were recorded and analyzed. After blood collection from patients, we used an immunocyte separation reagent kit to isolate immune cells, which were washed three times and stained with CD3 and CD56 molecules. The stained cells were analyzed using a flow cytometer, with a total of 1×10^5 immunocytes

recorded. Data recording and analysis were performed using the FlowJo software. Written informed consent was obtained from the families of all the study participants. This study was approved by the Ethics Committee of the Anhui Provincial Children's Hospital.

qRT-PCR detection of NK cell gene expression

NK cells were sorted by flow cytometry, and total RNA was extracted from the cells. RNA was heat-denatured at 65°C for 5 min and immediately placed on ice to cool. In the reaction system, 2 μL of 5x RT Master Mix and 1 μg of RNA template were added, followed by the addition of nuclease-free water to a final volume of 10 μL. The reaction mixture was gently mixed and subjected to reverse transcription at 37°C for 15 min, 50°C for 5 min, and 98°C for 5 min to obtain the cDNA template, which was then stored at 4°C. For qPCR, the resulting cDNA template was used in a 20 μL reaction system consisting of 6.4 μL distilled water, 10 μL SYBR® Green Realtime PCR Master Mix, 0.8 μL of each forward and reverse primer, and 2 μL of the sample. The mixture was then subjected to fluorescence quantitative PCR using a PCR machine with the following cycling conditions: 95°C for 30 s, followed by 40 cycles of 95°C for 5 s, 55°C for 10 s, and 72°C for 15 s. After amplification, the data were downloaded from the machine and processed. The primers used are listed in the table.

Statistical methods

Statistical analysis was conducted with SPSS 21.0 software. Continuous data were presented as mean ± standard deviation (SD). Comparisons between two independent groups were made using an independent samples t-test, while repeated measures analysis of variance was applied to repeated measured data. Categorical data were reported as counts or percentages, with the χ^2 test used for group comparisons. A *P*-value of less than 0.05 was considered to indicate statistical significance.

Results

Identification of genes associated with IBS-C and IBS-D

To identify genes associated with IBS-C and IBS-D, and genes in HV, we first obtained 113 differentially expressed up-regulated genes from GSE36701 with the screening conditions "p_adj < 0.05 and false discovery rate < 0.05". These DEGs are presented as a volcano plot. A heat map of the top 20 DEGs was plotted. Among them, in IBS-C-vs. HV, there were 51 upregulated genes (**Figure 1A**); in IBS-D vs. HV, there were 62 upregulated genes (**Figure 1A**); and in IBS-D vs. HV, there were 36 upregulated genes (**Figure 1A**). The differentially expressed genes common to pairwise comparisons were identified, revealing 24 shared up-regulated genes (**Figure 1B**). Only the top 20 are displayed in the heat map (**Figure 1C**).

Biological processes and pathways enriched for the Hub genes

Enrichment analyses were performed to elucidate the potential biological roles of these genes. Biological processes, including regulation of systemic processes, positive regulation of NADPH oxidase activity, and regulation of blood vessel endothelial cell proliferation, play a role in sprouting angiogenesis (**Figure 2A**). Cellular component analysis indicated that these genes were associated with integral components of intrinsic components of the membrane, plasma membrane, and intracellular non-membrane-bounded organelles (**Figure 2B**). The molecular function analysis revealed associations with positive regulation of endothelial cell proliferation, G protein-coupled peptide receptor activity, and regulation of steroid metabolic processes (**Figure 2C**). Twelve hub genes associated with IBS-C, IBS-D, and HV were identified by examining the intersections of 28 IBS-C vs. HV DEs and IBS-D vs. HV Des (**Figure 2D**). GO analysis revealed that two of the nine genes were involved in biological processes, including the regulation of steroid metabolic processes, angiotensin-activated signaling pathways, and renal sodium excretion (**Figure 2E**). Interactions between genes are represented by the protein-protein interaction (PPI) network (**Figure 2F**).

GSEA of hub genes

The respective functions of each gene were revealed by GSEA. The samples were categorized into two groups based on the median values of hub gene expression levels. The GSEA of these genes showed that they were associated with the glycosphingolipid biosynthesis ganglio series, base excision repair, and ribosomes (**Figure 3**).

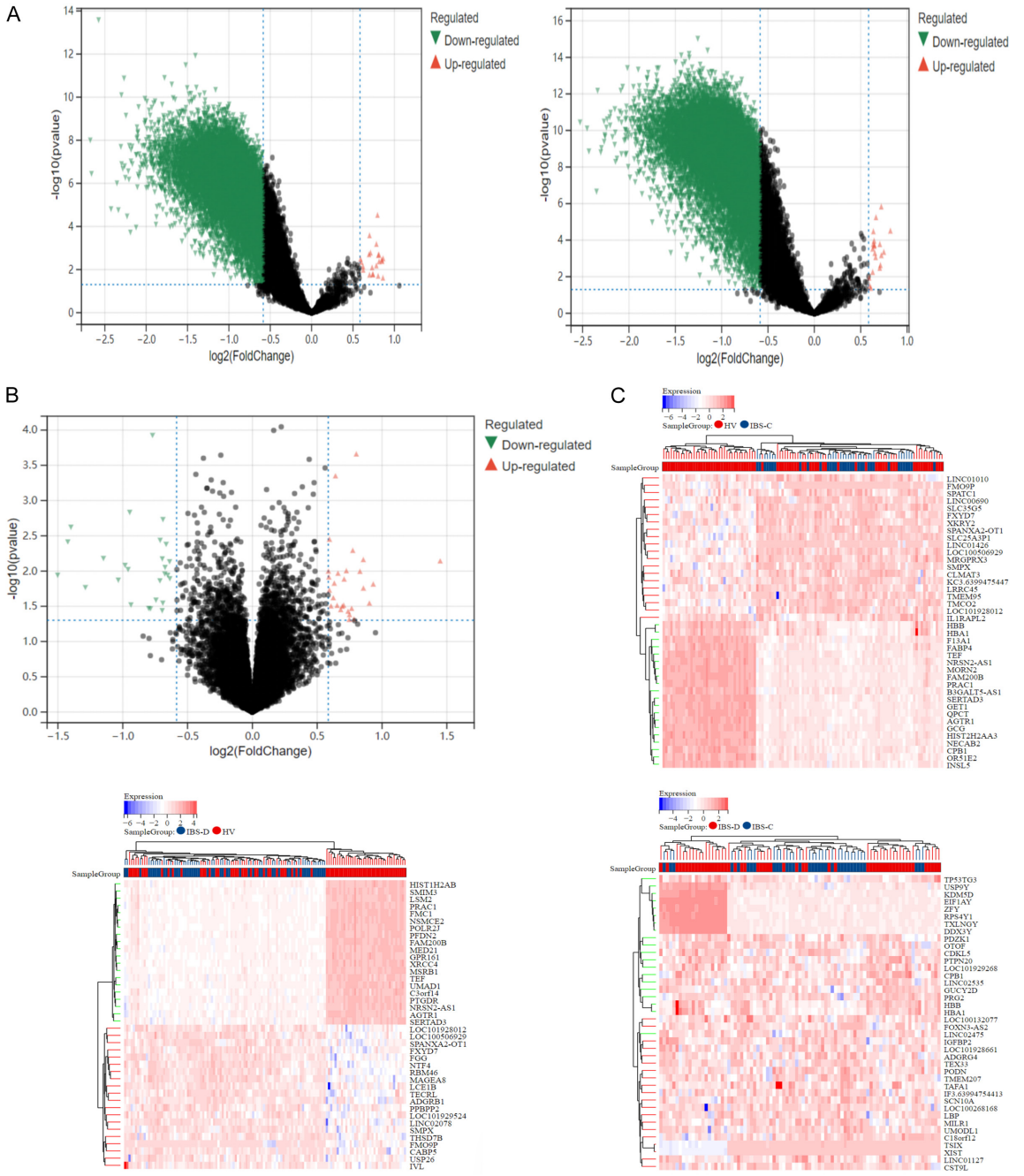

Figure 1. Differentially expressed genes associated with pediatric constipation versus healthy cohorts. A. Volcano plot of differentially expressed genes in IBS-C and HV groups. The red and green triangles in the volcano map represent differentially expressed genes from top to bottom. B. Volcano plot of common differentially expressed genes between IBS-C and HV groups. C. Heatmap of top 20 expressed genes (fold change) in each group.

Immune infiltration of TCGA of hub genes

Analysis of immune infiltration of The Cancer Genome Atlas (TCGA) of FAM200B, CD4⁺ shows negative correlation expression, while CD8⁺ shows positive correlation expression. In immune infiltration analysis of TCGA of FXYD7, both CD4⁺ and CD8⁺ showed positive correlation expression. In Immune infiltration analysis of TCGA of NRSN2, both CD4⁺ and CD8⁺ showed negative correlation expression. In Immune infiltration analysis of TCGA of

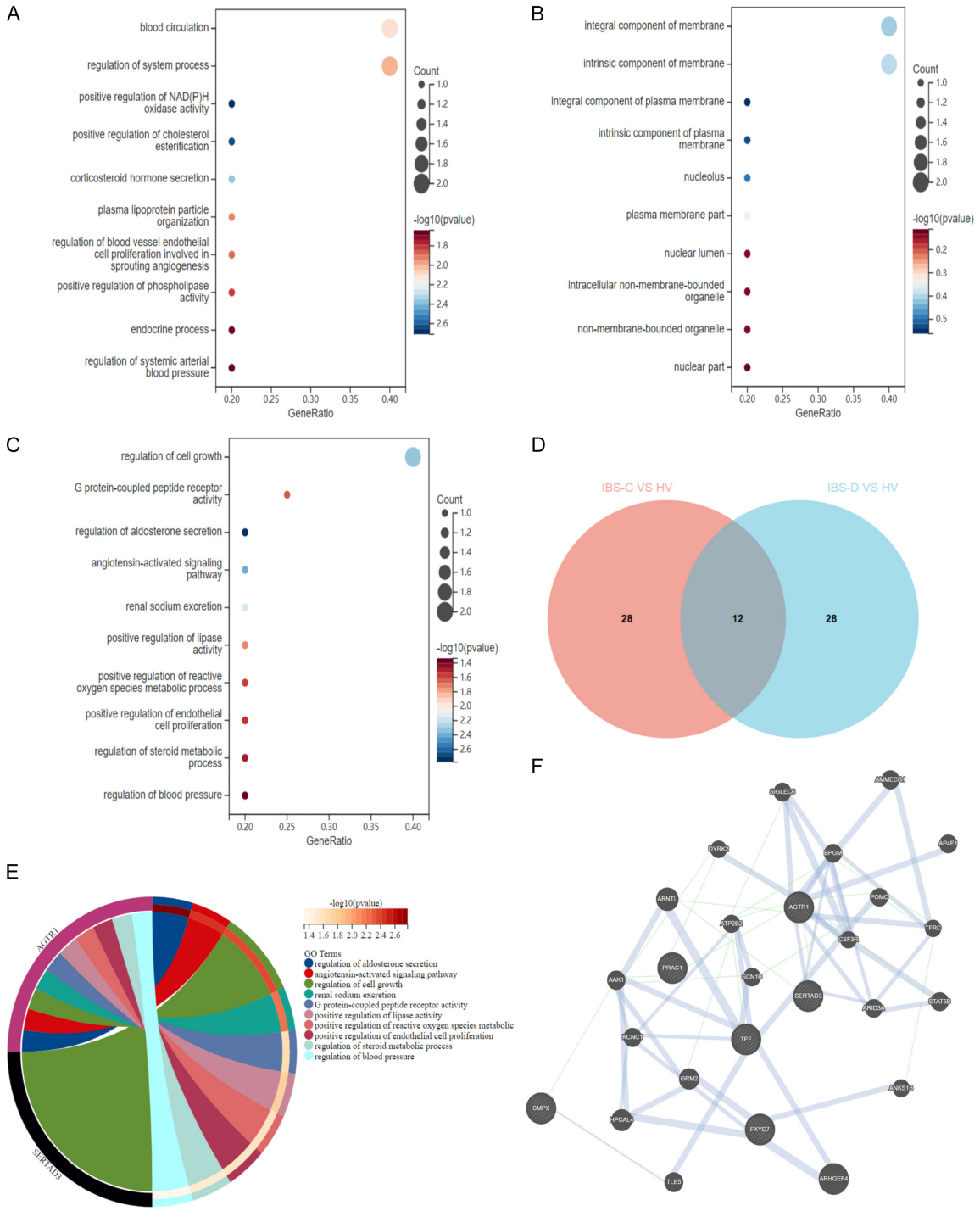

Figure 2. Functional enrichment study and PPI network of differentially expressed genes and hub genes related to the progression of constipation in children. A. Biological processes, including regulation of system process, positive regulation of NADPH oxidase activity. B. Cellular components, including integral component of intrinsic component of membrane. C. Molecular function, including positive regulation of endothelial cell proliferation, and G protein-coupled peptide receptor activity. D. The Venn plot shows the gene overlap between the differential genes of IBS-C vs. HV DEs, IBS-D vs. HV DEs. E. GO analysis. F. PPI Network.

SERTAD3 and SPANXA2, the expression patterns remain unclear. In Immune infiltration analysis of TCGA of TEF, CD4⁺ shows a negative correlation expression, while NK cells show a positive correlation expression (**Figure 4**).

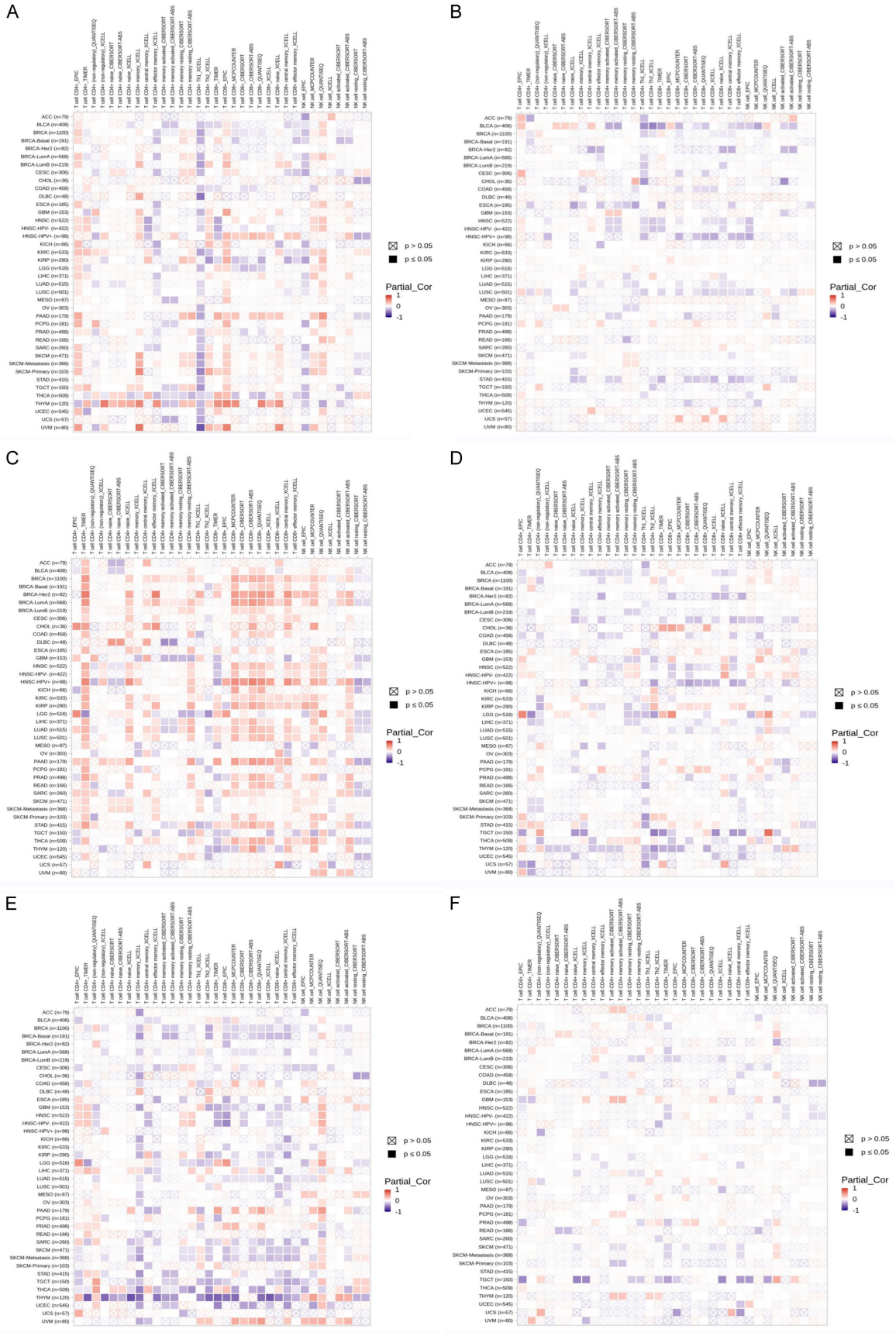
A
B
C
D
E
F
p > 0.05
p ≤ 0.05
Partial_Cor
1
0
-1

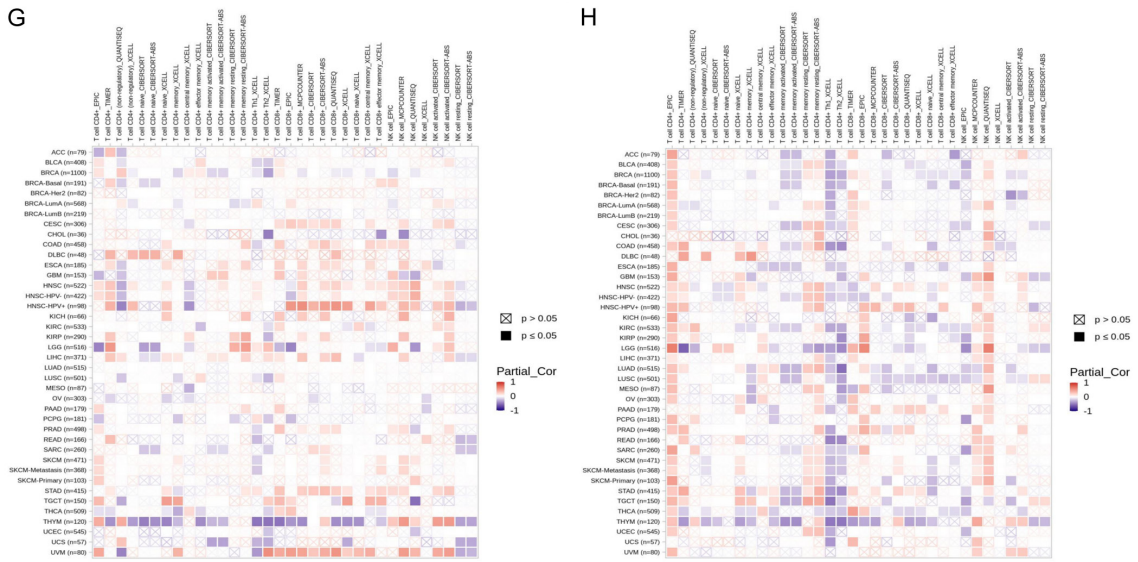

Figure 3. Pancancer immune infiltration expression of hub genes. Immune cell infiltration associated with the gene. A. FAM200B. B. FM09P. C. FXYD7. D. NRSN2. E. SERTAD3. F. SMPX. G. TEF. H. SPANXA2.

Construction and validation of a diagnostic model and immune infiltration of related genes

The tissue microenvironment consists of immune cells, the extracellular matrix, inflammatory factors, and various growth factors that have an important impact on clinical therapeutic sensitivity and disease diagnosis. In this study, the proportions of 22 immune cell types in 18 IBS-C, 27 IBS-D, and 40 HV samples were estimated using the CIBERSORT algorithm, as shown in the histogram (**Figure 5A**). Immune cell infiltration in IBS-C, IBS-D, and HV samples was compared using a boxplot (**Figure 5B**). The results showed that the HV group had significantly higher proportions of resting mast cells (P = 4.3e-6), activated NK cells (P = 0.01), and naive B cells (P = 1.3e-3), and lower proportions of activated mast cells (P = 4.4e-5) than the IBS-C and IBS-D groups.

A multigene prediction model was constructed using a logistic regression algorithm based on GSE36701. Using stepwise regression analysis, two of these nine genes, including AGTR1 and TEF, were selected to obtain the best model (**Figure 5C**). The findings revealed that the predictive model constructed from these two genes had good diagnostic performance, with an AUC of 0.74 (**Figure 5D**).

Significant decrease in CD56+ NK cell proportion in children with constipation

To validate the abnormalities in immune cells found in pediatric patients with constipation using bioinformatics, we examined the condition of immune cells in the blood of 20 patients and 20 healthy children. There were no significant differences in baseline data, such as sex, age, and blood cell composition, between the two groups of participants (**Table 1**). Subsequently, we isolated immune cells from the blood of the two participant groups and used flow cytometry to detect differences in their immune cell composition. The proportion of $CD3^+$ T cells did not differ between the two groups. $CD3^-$ cells were defined as the population of NK cells, and further differentiation was performed using CD56 expression in this group of cells. There was a significant difference in the expression of $CD56^+$ cells between the two groups (**Figure 6A**, **6B**). $CD56^+$ cells are usually considered mature NK cells, indicating abnormalities in NK cell maturation in CHC group.

Gene expression differences of NK cells in children with constipation

This study further examined the expression of hub genes in NK cells isolated from pediatric patients. The results revealed that in the CHC

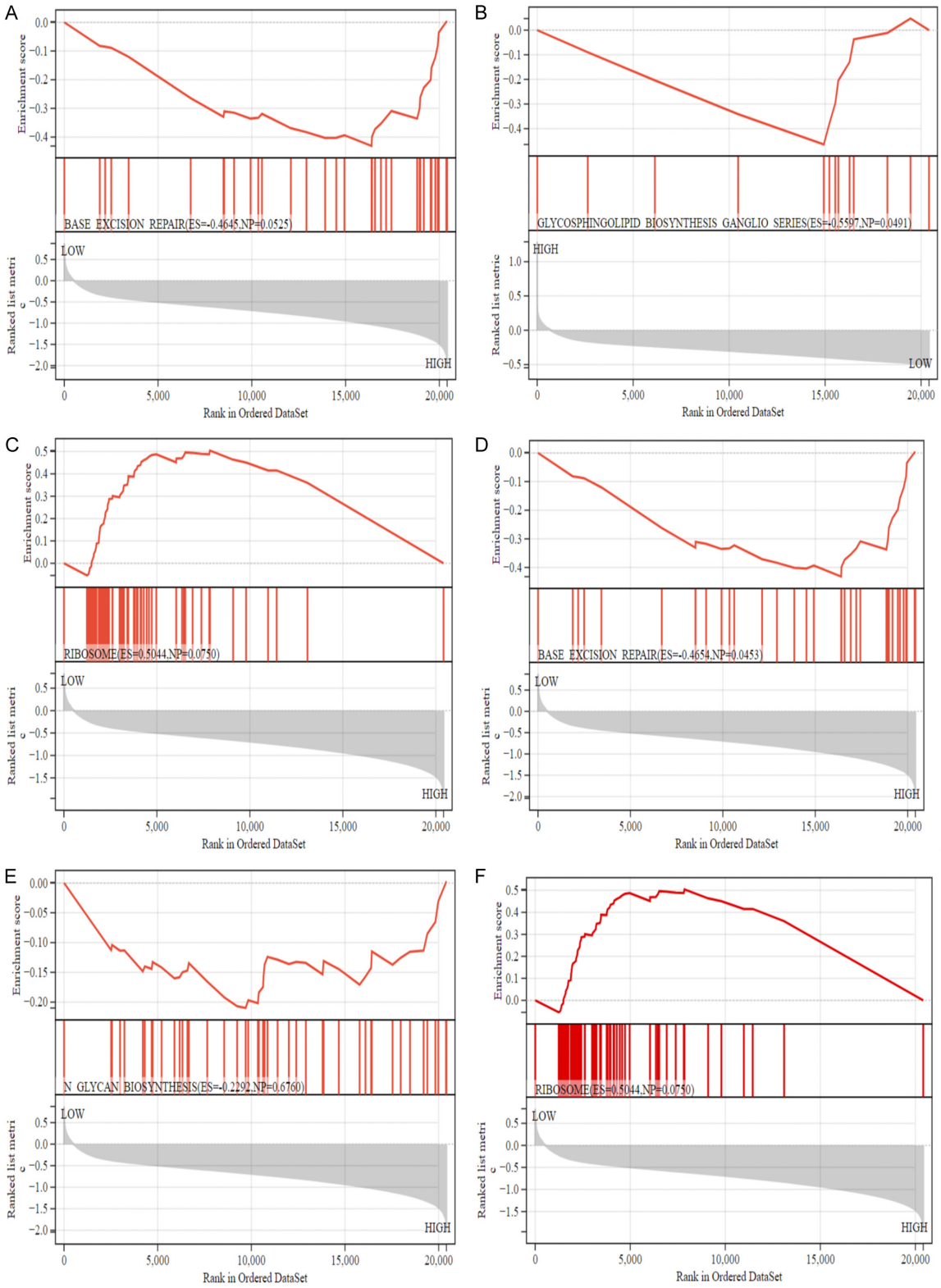

Figure 4. GSEA of hub genes. A. FAM200B. B. FXYD7. C. TEF. D. NRSN2-AS1. E. SMPX. F. SPANXA2.

group, the expression of AGTR1, FAM200B, NRSN2-AS1, PRAC1, SERTAD3, and TEF in NK cells isolated from the blood was lower compared to the HV group (**Figure 7A**). In contrast,

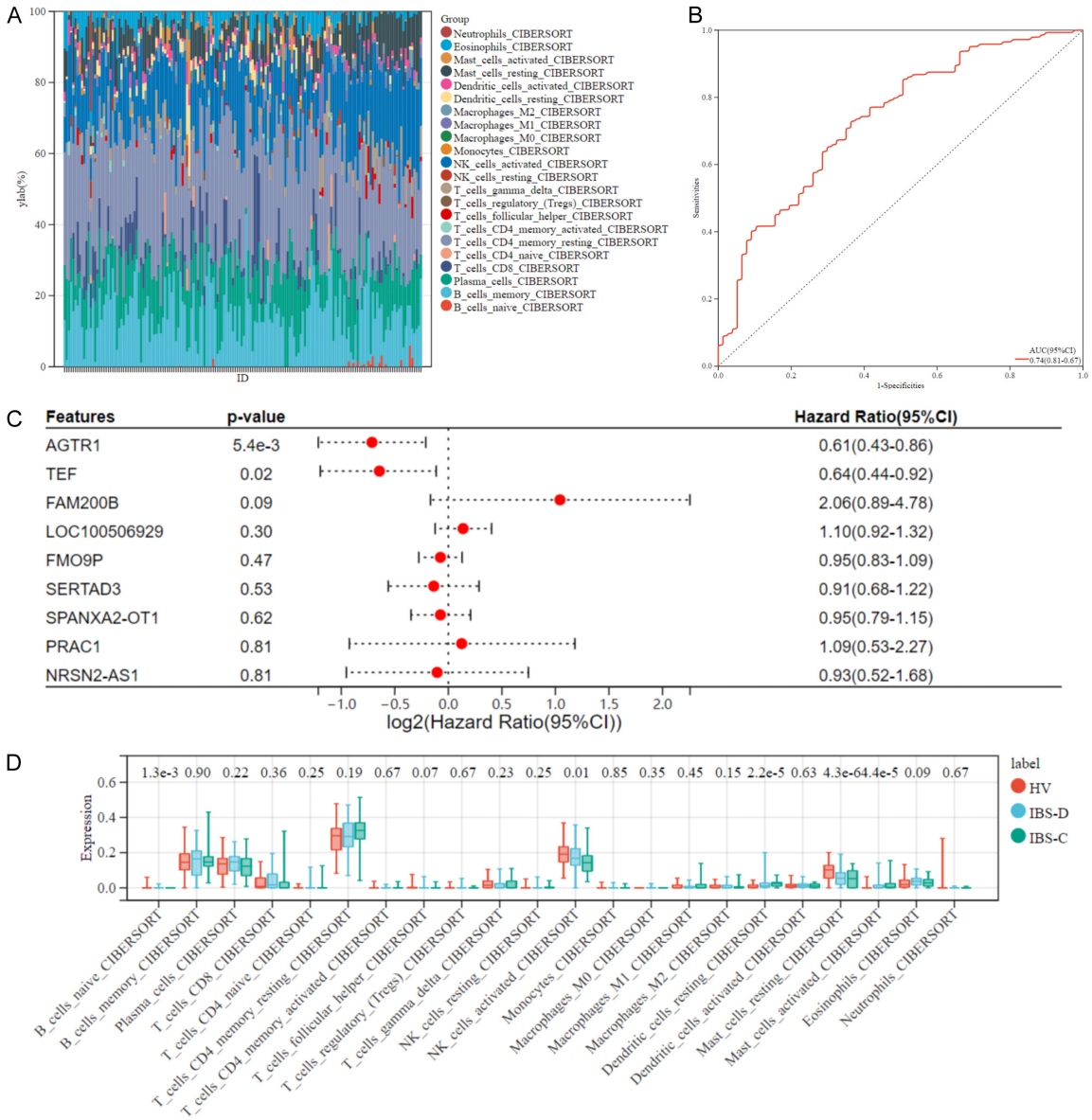

Figure 5. Construction and validation of a diagnostic model and immune infiltration of related genes. A. Proportion of immune cells in IBS-C, IBS-D and HV samples estimated by the CIBERSORT algorithm. B. predictive model with ROC curve. C. The proportion of immune cells in IBS-C, IBS-D and HV samples. D. Stepwise regression analysis of hub genes.

Table 1. Demographics and clinical characteristics of individuals

	HV (n = 20)	CHC (n = 20)
Female/Male	5/15	5/15
Mean Age (months)	69.8±35.7	58.1±47.6
WBC, ×10^9/L	14.0±1.8	7.27±1.6
RBC, g/L	125.3±6.8	118.1±23.4
PLT, ×10^9/L	287.5±53.1	295.4±100.9

WBC: white blood cells; RBC: red blood cells; PLT: platelets.

the expression levels of APANXA2-OT1, FMO9P, and LOC100506929 were higher in the CHC group compared to the HV group (**Figure 7B**). These differences in gene expression may play key roles in regulating the maturation of NK cells in pediatric patients with constipation.

Discussion

This study explored common core genes and pathways associated with pediatric constipa-

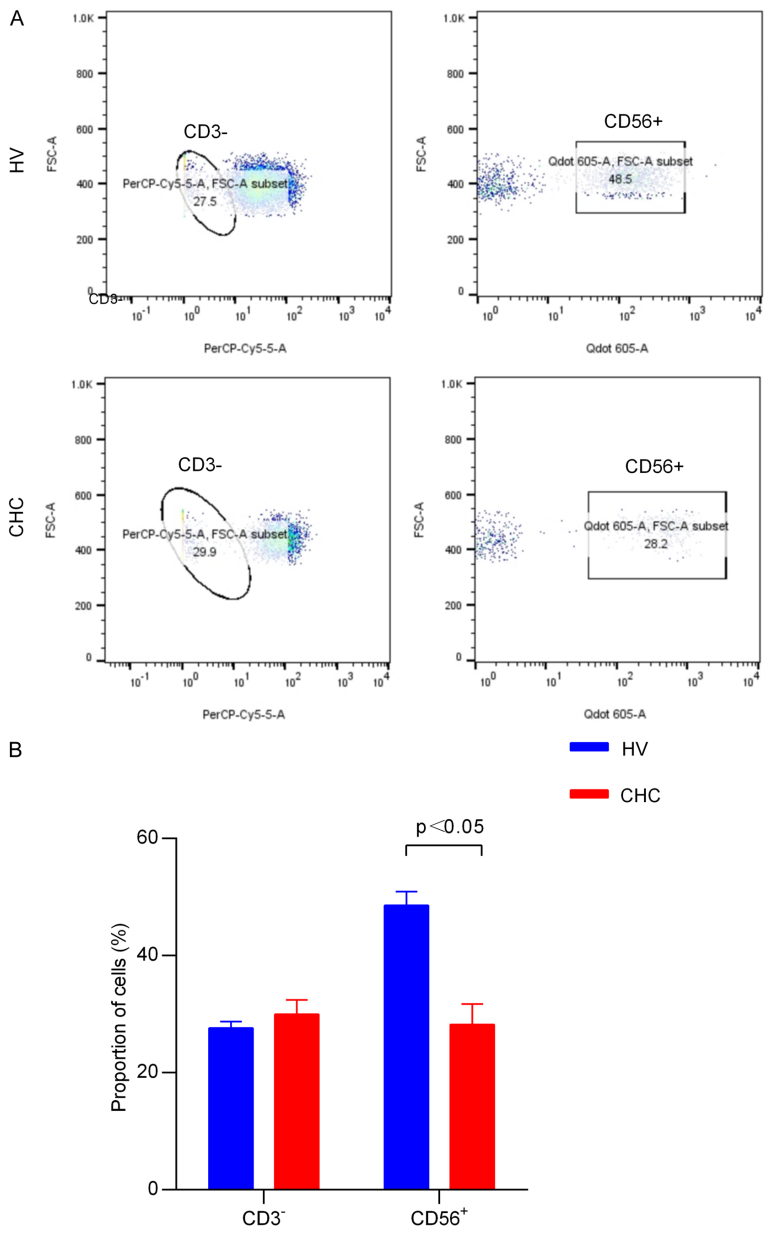

Figure 6. Flow cytometry detection of differences in immune cell subgroups and proportions between pediatric patients and healthy children. A. Subgroups and proportions of $CD3^-$ and $CD56^+$ cells in the two groups of children. B. Quantitative plot of the proportion of different cells (%).

tion and immune abnormalities using bioinformatic analysis of public databases. The identified genes were significantly upregulated in both CHC and patients with immune abnormalities. These genes were most strongly associated with the regulation of systemic processes, positive regulation of NADPH oxidase activity, and regulation of blood vessel endothelial cell proliferation involved in sprouting angiogenesis. Furthermore, GSEA analysis showed that many biological processes, including glycosphingolipid biosynthesis, ganglio series, base excision repair, and ribosomes, were associated with the high expression of these core genes.

In our subsequent studies on immune cell infiltration, we found differences in $CD4^+$ and $CD8^+$ T cells between normal individuals and children with CHC, as well as a higher percentage of $CD56^+$ NK cells in healthy individuals compared to children with CHC. Additionally, bioinformatics and flow cytometry analyses confirmed these findings regarding the differences in NK cells. Research has shown that the maturation of NK cells is significantly related to the expression intensity of CD56 on their surface, with $CD56^+$ NK cells considered mature and $CD56^-$ NK cells thought to be immature [21].

NK cells play a major role in the body's tissue immune defense, and their development and functional activity are regulated by multiple factors [22, 23]. During NK cell development, maturation can be assessed based on the expression levels of surface molecules [24, 25]. CD56 is an important marker of NK cells and can be used to distinguish between two subgroups of human NK cells, CD56bright and CD56dim. CD56bright NK cells express higher levels of CD56, CD16, and CD94, demonstrating strong cytotoxic and secretory functions. In contrast, CD56dim NK cells express lower levels of CD56, while showing higher levels of CD16 and NKG2A/C/E, primarily exhibiting cytotoxic characteristics [24, 26-28]. The low percentage of $CD56^+$ NK cells in CHC patients may be attributed to the toxic effects caused by constipation, which makes it difficult for NK cells to with-

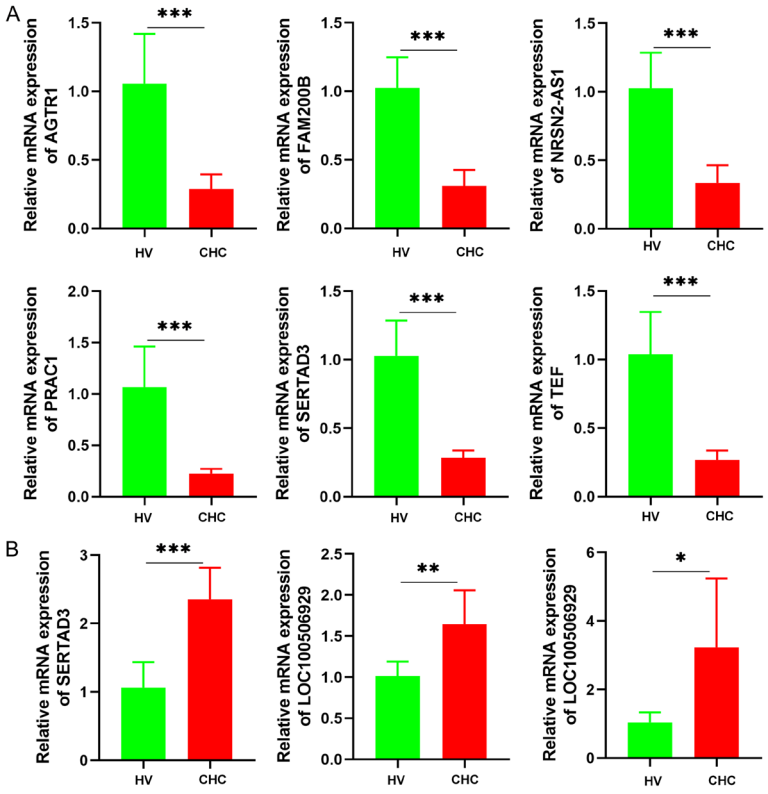

Figure 7. Detection of Hub gene expression in NK cells by qRT-PCR. A. Expression of AGTR1, FAM200B, NRSN2-AS1, PRAC1, SERTAD3, and TEF genes in the CHC group and HV group, ***P < 0.001 compared to the HV group. B. Expression of APANXA2-OT1, FMO9P, and LOC100506929 genes in the CHC group and HV group, ***P < 0.001, **P < 0.001 and *P < 0.05 compared to the HV group.

stand cytotoxicity [29]. Long-term constipation can lead to excessive accumulation of toxins and waste in the intestine, causing inflammatory reactions and immune system dysfunction [30]. These disruptions may impair various immune cell functions, including the development and maturation of NK cells [31]. However, further research is needed to elucidate the pathologic mechanisms of immune cells in pediatric constipation.

Acknowledgements

This project received funding support from the Anhui Provincial Department of Higher Education (Project No. 2022AH050447) and the Anhui Province Traditional Chinese Medicine Inheritance and Innovation Research Project (Project No. 2024CCCX130).

Disclosure of conflict of interest

None.

Address correspondence to: Yingying Wang, Department of Pediatrics, Anhui Provincial Children's Hospital, Hefei 230031, Anhui, P. R. China. E-mail: wyyetzyk@126.com; Lili Shang, Department of Pediatrics, The First Affiliated Hospital of Anhui University of Chinese Medicine, Hefei 230031, Anhui, P. R. China. E-mail: kyksh@126.com; Peisen Wang, Department of General Surgery, The First Affiliated Hospital of Anhui University of Chinese Medicine, Hefei 230031, Anhui, P. R. China. E-mail: yxq726116@126.com

References

[1] Bradshaw O, Foy R, Seal AK and Darling JC. Childhood constipation. BMJ 2021; 375: e065046.

[2] Loening-Baucke V. Prevalence, symptoms and outcome of constipation in infants and toddlers. J Pediatr 2005; 146: 359-63.

[3] Ho JMD and How CH. Chronic constipation in infants and children. Singapore Med J 2020; 61: 63-68.

[4] van den Berg MM, Benninga MA and Di Lorenzo C. Epidemiology of childhood constipation: a systematic review. Am J Gastroenterol 2006; 101: 2401-2409.

[5] Classen M, Righini-Grunder F, Schumann S, Gontard Av and Laffolie JD. Constipation in children and adolescents. Dtsch Arztebl Int 2022; 119: 697-708.

[6] Tran DL and Sintusek P. Functional constipation in children: What physicians should know. World J Gastroenterol 2023; 29: 1261-1288.

[7] Howard ER and Garrett JR. Chronic constipation in childhood. Lancet 1977; 2: 1237.

[8] Anderson JW, Baird P, Davis RH Jr, Ferreri S, Knudtson M, Koraym A, Waters V and Williams CL. Health benefits of dietary fiber. Nutr Rev 2009; 67: 188-205.

[9] Hojsak I, Benninga MA, Hauser B, Kansu A, Kelly VB, Stephen AM, Morais Lopez A, Slavin J and Tuohy K. Benefits of dietary fibre for children in health and disease. Arch Dis Child 2022; 107: 973-979.

[10] Muhardi L, Aw MM, Hasosah M, Ng RT, Chong SY, Hegar B, Toro-Monjaraz E, Darma A, Cetinkaya M, Chow CM, Kudla U and

Vandenplas Y. A narrative review on the update in the prevalence of infantile colic, regurgitation, and constipation in young children: implications of the ROME IV criteria. Front Pediatr 2022; 9: 778747.
[11] Saez A, Herrero-Fernandez B, Gomez-Bris R, Sánchez-Martinez H and Gonzalez-Granado JM. Pathophysiology of inflammatory bowel disease: innate immune system. Int J Mol Sci 2023; 24: 1526.
[12] Rose DR, Yang H, Careaga M, Angkustsiri K, Van de Water J and Ashwood P. T cell populations in children with autism spectrum disorder and co-morbid gastrointestinal symptoms. Brain Behav Immun Health 2020; 2: 100042.
[13] Domínguez-Andrés J, Dos Santos JC, Bekkering S, Mulder WJM, van der Meer JWM, Riksen NP, Joosten LAB and Netea MG. Trained immunity: adaptation within innate immune mechanisms. Physiol Rev 2023; 103: 313-346.
[14] Schnell A, Littman DR and Kuchroo VK. TH17 cell heterogeneity and its role in tissue inflammation. Nat Immunol 2023; 24: 19-29.
[15] Yan JB, Luo MM, Chen ZY and He BH. The function and role of the Th17/Treg cell balance in inflammatory bowel disease. J Immunol Res 2020; 2020: 8813558.
[16] Brockmann L, Tran A, Huang Y, Edwards M, Ronda C, Wang HH and Ivanov II. Intestinal microbiota-specific Th17 cells possess regulatory properties and suppress effector T cells via c-MAF and IL-10. Immunity 2023; 56: 2719-2735, e7.
[17] Renaude E, Kroemer M, Borg C, Peixoto P, Hervouet E, Loyon R and Adotévi O. Epigenetic reprogramming of CD4+ helper T cells as a strategy to improve anticancer immunotherapy. Front Immunol 2021; 12: 669992.
[18] Chen Y, Yu M, Liu X, Qu H, Chen Q, Qian W, Wei D, Xu W, Ma B and Wu W. Clinical characteristics and peripheral T cell subsets in Parkinson's disease patients with constipation. Int J Clin Exp Pathol 2015; 8: 2495-2504.
[19] Buckley MM, O'Mahony SM and O'Malley D. Convergence of neuro-endocrine-immune pathways in the pathophysiology of irritable bowel syndrome. World J Gastroenterol 2014; 20: 8846-8858.
[20] Peng Y, Ma Y, Luo Z, Jiang Y, Xu Z and Yu R. Lactobacillus reuteri in digestive system diseases: focus on clinical trials and mechanisms. Front Cell Infect Microbiol 2023; 13: 1254198.
[21] Poli A, Michel T, Thérésine M, Andrès E, Hentges F and Zimmer J. CD56bright natural killer (NK) cells: an important NK cell subset. Immunology 2009; 126: 458-465.
[22] Cooper MA, Fehniger TA and Caligiuri MA. The biology of human natural killer-cell subsets. Trends Immunol 2001; 22: 633-640.
[23] Cichocki F, Grzywacz B and Miller JS. Human NK cell development: one road or many? Front Immunol 2019; 10: 2078.
[24] Cocker ATH, Guethlein LA and Parham P. The CD56-CD16+ NK cell subset in chronic infections. Biochem Soc Trans 2023; 51: 1201-1212.
[25] Björkström NK, Strunz B and Ljunggren HG. Natural killer cells in antiviral immunity. Nat Rev Immunol 2022; 22: 112-123.
[26] Picard LK, Claus M, Fasbender F and Watzl C. Human NK cells responses are enhanced by CD56 engagement. Eur J Immunol 2022; 52: 1441-1451.
[27] Gianchecchi E, Delfino DV and Fierabracci A. NK cells in autoimmune diseases: linking innate and adaptive immune responses. Autoimmun Rev 2018; 17: 142-154.
[28] Kucuksezer UC, Aktas Cetin E, Esen F, Tahrali I, Akdeniz N, Gelmez MY and Deniz G. The role of natural killer cells in autoimmune diseases. Front Immunol 2021; 12: 622306.
[29] Chen S, Zhu H and Jounaidi Y. Comprehensive snapshots of natural killer cells functions, signaling, molecular mechanisms and clinical utilization. Signal Transduct Target Ther 2024; 9: 302.
[30] Lee SW, Park HJ, Van Kaer L and Hong S. Role of CD1d and iNKT cells in regulating intestinal inflammation. Front Immunol 2024; 14: 1343718.
[31] O'Brien KL and Finlay DK. Immunometabolism and natural killer cell responses. Nat Rev Immunol 2019; 19: 282-290.